On the Numerical Solution
of the Regularized Birkhoff Equations

By Christoph Börgers

Abstract. The Birkhoff equations for the evolution of vortex sheets are regularized in a way proposed by Krasny. The convergence of numerical approximations to a fixed regularization is studied theoretically and numerically. The numerical test problem is a two-dimensional inviscid jet.

1. Introduction. In [10] and [11], Krasny proposed and studied a method for the numerical computation of vortex sheet evolution. In this method, the Birkhoff equations [3] are regularized, and the regularized equations are then solved numerically.

The initial value problem for the Birkhoff equations is unstable. For analytic initial data, an analytic solution is known to exist for short time; cf. [14]. Numerical, asymptotic, and rigorous analysis have shown that the analyticity can be lost after a finite time; cf. [9], [13], and [6]. To prove the long-time existence of a weak solution is an open problem.

The regularized problem proposed by Krasny is well-posed. For short time, the convergence of solutions of the regularized problem to solutions of the original one has very recently been proved by Caflisch and Lowengrub [5].

We consider the numerical solution of the regularized equations. For a fixed regularization, we show the convergence of the numerical approximations. We show that this implies that the regularized sheets cannot self-intersect or intersect each other unless they do so at the initial time. Krasny expected this to be true, and used it as an accuracy check for his computations.

We also present a numerical accuracy study for the case of a pair of vortex sheets of equal strengths, opposite signs, periodic in the x-direction with period 1, and initially almost parallel. Such a pair of vortex sheets is a simple model of an inviscid jet. Flows of this kind have previously been studied by, e.g., Abernathy and Kronauer [1], Boldman, Brinich and Goldstein [4], Aref and Siggia [2], and Meiburg [12]. In [1] and [4], the point vortex method was used. Based on numerical evidence, it is now believed that this method does not converge past the critical time, i.e., the time of loss of analyticity; cf. [9]. Aref and Siggia [2] used the vortex-in-cell method. We have not yet compared the accuracy of their calculations with that of ours. The method in [12] is similar to Krasny's.

We ask the following question: Does one need an accurate computation of the details of the vortex sheet evolution in order to accurately determine global parameters associated with the flow, such as the momentum thickness? Our numerical experiments suggest that the answer is yes.

2. The Equations and Their Regularization. We consider inviscid, incompressible flow in two dimensions. Let the velocity field be $\mathbf{u}(\mathbf{x}, t)$, where $\mathbf{x}$ is a point in the plane, and $t \geq 0$ denotes the time. We shall always use the notation

$$(1) \qquad\qquad \mathbf{x} = (x, y)$$

for points in the plane. Similarly, we shall write

$$(2) \qquad\qquad \mathbf{u} = (u, v).$$

The vorticity ω is defined by

$$(3) \qquad\qquad \omega := \frac{\partial v}{\partial x} - \frac{\partial u}{\partial y}.$$

A line δ-distribution of vorticity is called a vortex sheet. In general, a line δ-distribution in the plane can be described by its support, which is a curve in the plane, and a strength function, which is a scalar function defined on the curve. In the case of a vortex sheet, we shall call this strength function the vorticity density.

We assume that the flow is periodic in the x-direction with period 1. Each of the sheets is connected and extends from $x = -\infty$ to $x = +\infty$. On any given sheet, the vorticity density is finite, nonzero, and of the same sign everywhere. Let $\sigma_i = 1$ if the ith sheet is positive, and $\sigma_i = -1$ if the ith sheet is negative. The total circulation per period on the ith sheet, i.e., the integral of the vorticity density over one period, is $\sigma_i \Gamma_i$, with $\Gamma_i > 0$.

The commonly used mathematical formulation of the problem is due to Birkhoff [3]. The vortex sheets are described by moving curves in the plane. The parametrization is such that the total amount of circulation between two points on a sheet is the difference between the corresponding curve parameters.

This results in the following initial value problem. Given curves

$$(4) \qquad\qquad \mathbf{x}_i^{(0)}(\gamma), \qquad \gamma \in R,$$

with

$$(5) \qquad\qquad \mathbf{x}_i^{(0)}(\gamma + \Gamma_i) \equiv \mathbf{x}_i^{(0)}(\gamma) + (1, 0)$$

and

$$(6) \qquad\qquad \frac{\partial \mathbf{x}_i^{(0)}}{\partial \gamma}(\gamma) \neq \mathbf{0} \quad \text{for all } \gamma,$$

find

$$(7) \qquad\qquad \mathbf{x}_i(\gamma, t), \qquad \gamma \in R, \ t \geq 0,$$

with

$$(8) \qquad\qquad \mathbf{x}_i(\gamma + \Gamma_i, t) \equiv \mathbf{x}_i(\gamma, t) + (1, 0),$$

$$(9) \qquad\qquad \frac{\partial \mathbf{x}_i}{\partial \gamma}(\gamma, t) \neq \mathbf{0} \quad \text{for all } \gamma \text{ and } t,$$

$$(10) \qquad \frac{\partial \mathbf{x}_i}{\partial t}(\gamma, t) \equiv \sum_{j=1}^{m} \sigma_j \int_0^{\Gamma_j} \mathbf{K}(\mathbf{x}_i(\gamma, t) - \mathbf{x}_j(\tilde{\gamma}, t)) \, d\tilde{\gamma},$$

and

$$(11) \qquad \mathbf{x}_i(\gamma, 0) \equiv \mathbf{x}_i^{(0)}(\gamma).$$

Here

$$(12) \qquad \mathbf{K}(x, y) := \frac{(-\sinh(2\pi y), \sin(2\pi x))}{2\cosh(2\pi y) - 2\cos(2\pi x)}$$

is the velocity field generated by an array of point vortices of unit strength located at the points $(k, 0)$, k integer, and the integrals in Eq. (10) are Cauchy principal values if $i = j$. These principal values exist because of the conditions (6) and (9), which express the finiteness of the sheet densities.

Krasny [10], [11] proposed replacing the kernel $\mathbf{K}$ by

$$(13) \qquad \mathbf{K}_\delta(x, y) := \frac{(-\sinh(2\pi y), \sin(2\pi x))}{2\cosh(2\pi y) - 2\cos(2\pi x) + 2\delta^2}.$$

The vorticity associated with this field is a regularization of the array of point vortices of unit strength at the locations $(k, 0)$, k integer. Numerical methods for the incompressible Euler or Navier-Stokes equations using regularizations of point vortices are called vortex blob methods; cf. [7]. We shall call $\mathbf{K}_\delta$ a periodic vortex blob.

The regularized equations are

$$(14) \qquad \frac{\partial \mathbf{x}_i}{\partial t}(\gamma, t) \equiv \sum_{j=1}^{m} \sigma_j \int_0^{\Gamma_j} \mathbf{K}_\delta(\mathbf{x}_i(\gamma, t) - \mathbf{x}_j(\tilde{\gamma}, t))\, d\tilde{\gamma}.$$

This regularization has no known physical interpretation, but it drastically simplifies the problem, both mathematically and numerically. The reason lies in the following observation.

LEMMA 1. *For any $\delta > 0$ and any multi-index $\alpha \in N^2$, there is a constant $C(\alpha, \delta)$ with*

$$(15) \qquad |D^\alpha \mathbf{K}_\delta(\mathbf{x})| \leq C(\alpha, \delta) \quad \text{for all } \mathbf{x}.$$

Proof. $\mathbf{K}_\delta$ is periodic in the x-direction,

$$(16) \qquad \mathbf{K}_\delta \to (\pm\tfrac{1}{2}, 0) \quad \text{as } y \to \pm\infty,$$

and

$$(17) \qquad |D^\alpha \mathbf{K}_\delta(x, y)| \leq C e^{-2\pi|y|}$$

for all multi-indices $\alpha \neq \mathbf{0}$, with C independent of (x, y). $\square$

From this, it is easy to conclude the existence, uniqueness and smoothness of solutions of the regularized initial value problem:

THEOREM 1. *Assume that the initial curves $\mathbf{x}_i^{(0)}$ are μ times continuously differentiable, $\mu \geq 0$. Then (8), (11), and (14) have a unique solution $(\mathbf{x}_1, \ldots, \mathbf{x}_m)$, and all derivatives*

$$(18) \qquad \frac{\partial^\nu}{\partial \gamma^\nu} \frac{\partial^\tau}{\partial t^\tau} \mathbf{x}_i(\gamma, t)$$

with $0 \leq \nu \leq \mu$ and $\tau \geq 0$ exist and are continuous.

Proof. Integrating Eq. (14) with respect to t, we obtain the fixed point equation

$$(19) \qquad \mathbf{x}_i(\gamma, t) \equiv \sum_{j=1}^{m} \sigma_j \int_0^t \int_0^{\Gamma_j} \mathbf{K}_\delta(\mathbf{x}_i(\gamma, \tilde{t}) - \mathbf{x}_j(\tilde{\gamma}, \tilde{t})) \, d\tilde{\gamma} \, d\tilde{t} + \mathbf{x}_i^{(0)}(\gamma).$$

Eqs. (14) and (19) are equivalent. Let $T > 0$. Let B_T denote the Banach space of all m-tuples $(\mathbf{x}_i(\gamma, t))_{1 \le i \le m}$ with $\gamma \in R$ and $t \in [0, T]$ which satisfy Eq. (8) and are continuous in γ and t and μ times continuously differentiable with respect to γ. The right-hand side of Eq. (19) is a continuous operator $B_T \to B_T$. From Lemma 1 it follows that this operator is contracting as long as T is smaller than some $T_{\max}$ independent of the initial data $\mathbf{x}_i^{(0)}$. The Banach fixed point theorem then implies the existence of a unique solution defined for, say, $t \in [0, T_{\max}/2]$, which is μ times continuously differentiable with respect to γ. Since $T_{\max}$ does not depend on $(\mathbf{x}_i^{(0)})_{0 \le i \le m}$, repeated application of this argument shows the existence of a unique solution defined for all time which is μ times continuously differentiable with respect to γ. From Eq. (14) it now follows that

$$(20) \qquad \frac{\partial \mathbf{x}_i}{\partial t}(\gamma, t)$$

is μ times continuously differentiable with respect to γ. Through repeated differentiation of Eq. (14), one finds by induction that all time derivatives of $\mathbf{x}_i$ are μ times continuously differentiable with respect to γ. $\square$

It is natural to ask whether the solution is analytic if the initial curves are analytic. Although this question is of little importance for the main issue which we want to study, namely the numerical solution of the regularized equations, we note that the answer is yes. This result was proved independently by Caflisch and Lowengrub (Theorem 1 in [5]).

THEOREM 2. *Assume that the initial curves $\mathbf{x}_i^{(0)}$ are real analytic. Then the unique solution $(\mathbf{x}_1, \ldots, \mathbf{x}_m)$ of (8), (11), and (14) is real analytic in γ for all $t \ge 0$.*

Outline of Proof. Let $t > 0$ be arbitrary, but fixed. Consider Euler's method for the solution of Eq. (14) up to time t, leaving the integrals in Eq. (14) undiscretized, with a time step size $\Delta t = t/k$, k integer:

$$(21) \qquad \begin{aligned} \mathbf{x}_{i,\Delta t}(\gamma, (\nu + 1)\Delta t) &= \mathbf{x}_{i,\Delta t}(\gamma, \nu \Delta t) \\ &+ \Delta t \sum_{j=1}^{m} \sigma_j \int_0^{\Gamma_j} \mathbf{K}_\delta(\mathbf{x}_{i,\Delta t}(\gamma, \nu \Delta t) - \mathbf{x}_{j,\Delta t}(\tilde{\gamma}, \nu \Delta t)) \, d\tilde{\gamma} \end{aligned}$$

for $\nu = 0, \ldots, k - 1$.

The usual proof of convergence for Euler's method [8, p. 11] is applicable and shows

$$(22) \qquad \mathbf{x}_{i,\Delta t}(\gamma, t) \to \mathbf{x}_i(\gamma, t)$$

uniformly in γ. The approximations $\mathbf{x}_{i,\Delta t}(\gamma, t)$ obtained by Euler's method are easily seen to be real analytic in γ, since $\mathbf{K}_\delta(x, y)$ is an analytic function of the two complex variables x and y. Thus, the $\mathbf{x}_{i,\Delta t}(\gamma, t)$ have analytic extensions into open neighborhoods U_i of $[0, \Gamma_i]$ in the complex plane. U_i might depend on Δt, because $\mathbf{K}_\delta(x, y)$ is not defined for all complex x, y. However, differentiating Eq. (21)

with respect to the complex argument γ, a straightforward estimate shows that the complex derivatives of $\mathbf{x}_{i,\Delta t}(\gamma, t)$ are bounded independently of Δt. This implies that the neighborhoods U_i can be chosen independently of Δt. Again applying the proof of convergence for Euler's method, now with complex $\gamma \in U_i$, we find that for $\Delta t \to 0$, i.e., $k \to \infty$,

$$(23) \qquad\qquad \mathbf{x}_{i,\Delta t}(\gamma, t) \to \mathbf{x}_i(\gamma, t)$$

uniformly in $\gamma \in U_i$. This proves the assertion, since uniform limits of holomorphic functions are holomorphic. $\quad\square$

In summary, the initial value problem for the regularized equations has a unique solution which is as smooth as the initial data.

3. The Space Discretized Equations. We discretize the integrals in Eq. (14) using the trapezoidal rule. We call the resulting system of ordinary differential equations the space discretized problem. The mesh for the ith sheet has N_i points per period. The mesh points in $(0, \Gamma_i]$ are

$$(24) \qquad\qquad 0 < \gamma_1^{(i)} < \gamma_2^{(i)} < \cdots < \gamma_{N_i}^{(i)} = \Gamma_i.$$

We set

$$(25) \qquad\qquad \gamma_0^{(i)} := 0.$$

The space discretized equations then are

$$(26) \qquad \frac{\partial \mathbf{x}_i^h}{\partial t}(\gamma, t) \equiv \sum_{j=1}^m \sigma_j \sum_{\nu=1}^{N_j} \frac{(\gamma_\nu^{(j)} - \gamma_{\nu-1}^{(j)})}{2} [\mathbf{K}_\delta(\mathbf{x}_i^h(\gamma, t) - \mathbf{x}_j^h(\gamma_{\nu-1}^{(j)}, t))$$
$$+ \mathbf{K}_\delta(x_i^h(\gamma, t) - \mathbf{x}_j^h(\gamma_\nu^{(j)}, t))].$$

In a practical computation, $\mathbf{x}_i^h(\gamma, t)$ is determined only for $\gamma = \gamma_\nu^{(i)}$, $\nu = 1, \ldots, N_i$. However, Eq. (26) defines $\mathbf{x}_i^h(\gamma, t)$ for all $\gamma \in R$.

THEOREM 3. *Assume that the initial curves* $\mathbf{x}_j^{(0)}$ *are μ times continuously differentiable, $\mu \geq 0$. Then (8), (11), and (26) have a unique solution $(\mathbf{x}_1^h, \ldots, \mathbf{x}_m^h)$, and all derivatives*

$$(27) \qquad\qquad \frac{\partial^\nu}{\partial \gamma^\nu} \frac{\partial^\tau}{\partial t^\tau} \mathbf{x}_i^h(\gamma, t)$$

with $0 \leq \nu \leq \mu$ and $\tau \geq 0$ exist and are continuous.

Proof. Analogous to the proof of Theorem 1. $\quad\square$

4. Convergence, Not Including the Time Discretization. When the trapezoidal rule is applied to a periodic integrand, the order of convergence only depends on the smoothness of the integrand. From this, we shall now derive corresponding estimates for the convergence of the curves $\mathbf{x}_i^h$ to $\mathbf{x}_i$.

We set

$$(28) \qquad\qquad h_j := \max_\nu (\gamma_\nu^{(j)} - \gamma_{\nu-1}^{(j)})$$

and

$$(29) \qquad\qquad h := \max_j h_j.$$

We use the notation $\|\mathbf{x}\|$ for the Euclidean norm of a vector $\mathbf{x}$.

THEOREM 4. *Assume that the initial curves $x_j^{(0)}$ are μ times continuously differentiable, $\mu \geq 1$. Set*

$$(30) \qquad \mu_0 := \mu$$

if the meshes are equidistant, i.e., if

$$(31) \qquad \gamma_\nu^{(j)} - \gamma_{\nu-1}^{(j)} = h_j \quad \text{for all } \nu;$$

otherwise,

$$(32) \qquad \mu_0 := \min(\mu, 2).$$

For $t \geq 0$, let

$$(33) \qquad e(h,t) := \max_i \max_\gamma \|\mathbf{x}_i(\gamma, t) - \mathbf{x}_i^h(\gamma, t)\|.$$

Let $T > 0$. Then there are constants $C = C(T, \mu, \delta, m)$ and $L = L(\delta, m)$ such that

$$(34) \qquad e(h,t) \leq \frac{C}{L}(e^{Lt} - 1)h^{\mu_0}$$

for all $t \in [0, T]$.

Proof. Using obvious notational conventions, we abbreviate Eq. (14) by

$$(35) \qquad \frac{\partial \mathbf{x}_i}{\partial t} = \sum_{j=1}^m I(\mathbf{x}_i, \mathbf{x}_j),$$

and Eq. (26) by

$$(36) \qquad \frac{\partial \mathbf{x}_i^h}{\partial t} = \sum_{j=1}^m I^{h_j}(\mathbf{x}_i^h, \mathbf{x}_j^h).$$

We set

$$(37) \qquad \mathbf{e}_i^h(\gamma, t) := \mathbf{x}_i(\gamma, t) - \mathbf{x}_i^h(\gamma, t).$$

Then

$$(38) \qquad \frac{\partial \mathbf{e}_i^h}{\partial t} = \sum_{j=1}^m (I(\mathbf{x}_i, \mathbf{x}_j) - I^{h_j}(\mathbf{x}_i, \mathbf{x}_j)) + \sum_{j=1}^m (I^{h_j}(\mathbf{x}_i, \mathbf{x}_j) - I^{h_j}(\mathbf{x}_i^h, \mathbf{x}_j^h)).$$

Integrating this from 0 to t, using the convergence estimate for the trapezoidal rule for periodic integrands for the first sum in (38), and using the global Lipschitz continuity of $\mathbf{K}_\delta$ for the second sum in (38), we find

$$(39) \qquad e(h,t) \leq Cth^{\mu_0} + L \int_0^t e(h, \tau)\, d\tau$$

for some $L = L(\delta, m)$. Using Gronwall's lemma (that is, integrating Eq. (39)), we obtain

$$(40) \qquad e(h,t) \leq \frac{C}{L}(e^{Lt} - 1)h^{\mu_0}$$

for all $t \in [0, T]$. $\square$

THEOREM 5. *Assume that the initial curves* $\mathbf{x}_j^{(0)}$ *are real analytic, and that the meshes are equidistant. Then there are constants* $C = C(T, \mu, \delta, m)$ *and* $L = L(\delta, m)$ *such that*

$$(41) \qquad e(h, t) \leq \frac{1}{L}(e^{Lt} - 1)e^{-C/h}$$

for all $t \in [0, T]$.

Proof. Analogous to the proof of Theorem 4, using Theorem 2. □

5. Self-Intersections and Intersections of Vortex Sheets with Each Other. In this section we explain why the vortex sheets cannot self-intersect or intersect each other unless they do so for all t.

THEOREM 6. *Assume that there are no intersections in the initial sheets, i.e.,*

$$(42) \qquad \mathbf{x}_i^{(0)}(\gamma) = \mathbf{x}_j^{(0)}(\tilde{\gamma}) \Rightarrow i = j \quad and \quad \gamma = \tilde{\gamma}.$$

Then for all $t \geq 0$,

$$(43) \qquad \mathbf{x}_i(\gamma, t) = \mathbf{x}_j(\tilde{\gamma}, t) \Rightarrow i = j \quad and \quad \gamma = \tilde{\gamma}.$$

Proof. Suppose that for some $T > 0$,

$$(44) \qquad \mathbf{x}_i(\gamma_*, T) = \mathbf{x}_j(\tilde{\gamma}_*, T),$$

$i \neq j$ or $\gamma_* \neq \tilde{\gamma}_*$. We consider a sequence of m-tuples of meshes covering $[0, \Gamma_1], \ldots, [0, \Gamma_m]$ such that $h \to 0$, and such that γ_* is always a point in the ith mesh, and $\tilde{\gamma}_*$ is always a point in the jth mesh.

Consider the space discretized equations (26), with γ now restricted to the mesh $\{\gamma_1^{(i)}, \ldots, \gamma_{N_i}^{(i)}\}$. (26) is then a system of ordinary differential equations describing the motion of N points ξ_k, $k = 1, \ldots, N$, in the plane, with

$$(45) \qquad N := N_1 + \cdots + N_m.$$

The system is of the form

$$(46) \qquad \frac{d\xi_k}{dt} = \sum_l \omega_l \mathbf{K}_\delta(\xi_k - \xi_l).$$

We note that

$$(47) \qquad \sum_{\nu=1}^{N} |\omega_\nu| = \sum_{j=1}^{m} \Gamma_j.$$

Let $L > 0$ with

$$(48) \qquad \|\mathbf{K}_\delta(\xi) - \mathbf{K}_\delta(\tilde{\xi})\| \leq L\|\xi - \tilde{\xi}\| \quad \text{for all } \xi, \tilde{\xi}.$$

There is such a constant L by Lemma 1. From (46), it follows that

$$(49) \qquad \frac{d}{dt}\|\xi_k(t) - \xi_l(t)\|^2 \leq 2L\left(\sum_{\nu=1}^{N} |\omega_\nu|\right)\|\xi_k(t) - \xi_l(t)\|^2.$$

Integrating and applying Gronwall's lemma, we find for all $t \geq 0$:

$$(50) \qquad \|\xi_k(t) - \xi_l(t)\| \leq e^{L(\sum_{\nu=1}^{N} |\omega_\nu|)t}\|\xi_k(0) - \xi_l(0)\|.$$

The analogous estimate holds for the backward equation, which implies that also

$$
(51) \qquad \|\boldsymbol{\xi}_k(t) - \boldsymbol{\xi}_l(t)\| \geq e^{-L(\sum_{\nu=1}^{N} |\omega_\nu|)t} \|\boldsymbol{\xi}_k(0) - \boldsymbol{\xi}_l(0)\|,
$$

thus, using Eq. (47),

$$
(52) \qquad \|\boldsymbol{\xi}_k(t) - \boldsymbol{\xi}_l(t)\| \geq e^{-L(\sum_{j=1}^{m} \Gamma_j)t} \|\boldsymbol{\xi}_k(0) - \boldsymbol{\xi}_l(0)\|.
$$

Thus, the two points which, by our assumption, collide at time T in the continuous case, stay bounded away from each other by their initial separation times

$$
(53) \qquad e^{-L(\sum_{j=1}^{m} \Gamma_j)T}
$$

in the discrete case. This contradicts Theorem 4. ◻

6. Convergence, Including the Time Discretization. Suppose that the equations (26) are solved with the classical fourth-order Runge-Kutta method with a fixed step size $\Delta t > 0$, as in [10], [11]. We denote the resulting approximation by $\mathbf{x}_i^h(\gamma, t, \Delta t)$, defined for all γ, but only for $t = 0, \Delta t, 2\Delta t, \ldots$. From the convergence estimate for the Runge-Kutta method it follows that for $0 \leq t \leq T$,

$$
(54) \qquad \|\mathbf{x}_i(\gamma, t) - \mathbf{x}_i^h(\gamma, t, \Delta t)\| \leq Ch^{\mu_0} + D\Delta t^4,
$$

with

$$
(55) \qquad C = C(T, \mu, \delta, m)
$$

and

$$
(56) \qquad D = D(T, \delta, h).
$$

THEOREM 7. *D can be chosen independently of h.*

Proof. This is a consequence of the following estimate:

$$
(57) \qquad \left\| \frac{\partial^\tau}{\partial t^\tau} \mathbf{x}^h(\gamma, t) \right\| \leq C
$$

for a constant C which depends on T, δ, τ, but not on h, γ and $t \in [0, T]$.

For $\tau = 0$, (57) follows from the uniform convergence $\mathbf{x}^h \to \mathbf{x}$. For $\tau > 0$, it follows by induction on τ, using the space discretized equations (26) and their time derivatives. ◻

The bound C in (57) tends to ∞ as $\delta \to 0$. Therefore, we expect that small values of δ will require small time steps. This can be confirmed through numerical experiments.

7. The Regularized Equations for a Shifted Symmetric Jet. We now consider the case of two vortex sheets of opposite signs. The sheets are now denoted by

$$
(58) \qquad \mathbf{x}_+(\gamma, t), \qquad \gamma \in [0, \Gamma],
$$

and

$$
(59) \qquad \mathbf{x}_-(\gamma, t), \qquad \gamma \in [0, \Gamma].
$$

$\mathbf{x}_+$ has the vorticity $\Gamma > 0$ per period, and $\mathbf{x}_-$ has the vorticity $-\Gamma$ per period. If the curves (58), (59) solve the regularized equations, and if for $t = 0$,

(60)
$$x_+(\gamma, t) \equiv x_-(\gamma, t) + \tfrac{1}{2}$$

and

(61)
$$y_+(\gamma, t) \equiv -y_-(\gamma, t),$$

then (60) and (61) hold for all $t \geq 0$. This follows from the uniqueness of the solution of the initial value problem for the regularized Birkhoff equations. If (60) and (61) hold, we say that $\mathbf{x}_+$ and $\mathbf{x}_-$ describe a *shifted symmetric* jet. We use the notation

(62)
$$\mathbf{x} := \mathbf{x}_+,$$

and, as before,

(63)
$$\mathbf{x} = (x, y).$$

From the general regularized Birkhoff equations (14), together with the shifted symmetry conditions (60) and (61), we obtain

(64)
$$\frac{\partial x}{\partial t} = -\frac{1}{2} \int_0^\Gamma \frac{\sinh(2\pi(y - \tilde{y}))}{\cosh(2\pi(y - \tilde{y})) - \cos(2\pi(x - \tilde{x})) + \delta^2} \, d\tilde{\gamma}$$
$$+ \frac{1}{2} \int_0^\Gamma \frac{\sinh(2\pi(y + \tilde{y}))}{\cosh(2\pi(y + \tilde{y})) + \cos(2\pi(x - \tilde{x})) + \delta^2} \, d\tilde{\gamma},$$

and

(65)
$$\frac{\partial y}{\partial t} = \frac{1}{2} \int_0^\Gamma \frac{\sin(2\pi(x - \tilde{x}))}{\cosh(2\pi(y - \tilde{y})) - \cos(2\pi(x - \tilde{x})) + \delta^2} \, d\tilde{\gamma}$$
$$+ \frac{1}{2} \int_0^\Gamma \frac{\sin(2\pi(x - \tilde{x}))}{\cosh(2\pi(y + \tilde{y})) + \cos(2\pi(x - \tilde{x})) + \delta^2} \, d\tilde{\gamma},$$

where x, y stand for $x(\gamma, t)$, $y(\gamma, t)$, and $\tilde{x}$, $\tilde{y}$ stand for $x(\tilde{\gamma}, t)$, $y(\tilde{\gamma}, t)$. Equations (64) and (65), together with an initial condition

(66)
$$\mathbf{x}(\gamma, t) \equiv \mathbf{x}^{(0)}(\gamma),$$

determine $\mathbf{x}(\gamma, t)$ for all $\gamma \in R$ and $t \geq 0$. For all t, $\mathbf{x}(\gamma, t)$ is as smooth as $\mathbf{x}^{(0)}(\gamma)$.

8. The Discretized Equations for a Shifted Symmetric Jet.

The integrals in Eqs. (64) and (65) are discretized using the trapezoidal rule with a fixed mesh size $\frac{\Gamma}{N}$, N integer. The resulting ordinary differential equations, the space discretized equations, are

(67)
$$\frac{dx_i}{dt} = -\frac{\Gamma}{2N} \sum_{j=1}^N \frac{\sinh(2\pi(y_i - y_j))}{\cosh(2\pi(y_i - y_j)) - \cos(2\pi(x_i - x_j)) + \delta^2}$$
$$+ \frac{\Gamma}{2N} \sum_{j=1}^N \frac{\sinh(2\pi(y_i + y_j))}{\cosh(2\pi(y_i + y_j)) + \cos(2\pi(x_i - x_j)) + \delta^2}$$

and

$$
\begin{aligned}
(68) \quad \frac{dy_i}{dt} = {} & \frac{\Gamma}{2N} \sum_{j=1}^{N} \frac{\sin(2\pi(x_i - x_j))}{\cosh(2\pi(y_i - y_j)) - \cos(2\pi(x_i - x_j)) + \delta^2} \\
& + \frac{\Gamma}{2N} \sum_{j=1}^{N} \frac{\sin(2\pi(x_i - x_j))}{\cosh(2\pi(y_i + y_j)) + \cos(2\pi(x_i - x_j)) + \delta^2}.
\end{aligned}
$$

$x_i(t)$ and $y_i(t)$ are approximations for $x(\frac{i\Gamma}{N})$ and $y(\frac{i\Gamma}{N})$. As before, Eqs. (67), (68) are solved using the classical fourth-order Runge-Kutta method with step size Δt.

9. The Momentum thickness. Let

$$
(69) \qquad \mathbf{u}(\mathbf{x}, t) = (u(x, y, t), v(x, y, t))
$$

be a two-dimensional velocity field, with

$$
(70) \qquad \mathbf{u}(x + 1, y, t) \equiv \mathbf{u}(x, y, t).
$$

The *x-momentum thickness* of $\mathbf{u}$ at time t is

$$
(71) \qquad \theta(t) := \frac{\int_{-\infty}^{\infty} [\bar{u}(y, t) - \bar{u}(\infty, t)]\, dy}{\bar{u}(0, t) - \bar{u}(\infty, t)},
$$

where $\bar{u}$ denotes the x-average of u over one period. We assume that $\bar{u}(-\infty, t) \equiv \bar{u}(\infty, t)$.

To motivate this definition, let $x = x^*$ and $t = t^*$ be fixed. Assume that the time unit and coordinate system are such that $u(x^*, 0, t^*) = 1$ and $u(x^*, \infty, t^*) = u(x^*, -\infty, t^*) = 0$. Assume that $\mathbf{u}$ is the velocity field of a fluid with density one. Then

$$
(72) \qquad \frac{\int_{-\infty}^{\infty} [u(x^*, y, t^*) - u(x^*, \infty, t^*)]\, dy}{u(x^*, 0, t^*) - u(x^*, \infty, t^*)} = \int_{-\infty}^{\infty} u(x^*, y, t^*)\, dy
$$

is the amount of fluid crossing the line $x \equiv x^*$ in unit time. If the flow under consideration is a jet, this amount of fluid is a measure of "thickness". Thus $\theta(t)$ can be regarded as the average thickness of the jet at time t.

Let

$$
(73) \qquad \mathbf{u}_{(x_0, y_0)}(x, y) := \frac{(-\sinh(2\pi(y - y_0)), \sin(2\pi(x - x_0)))}{2\cosh(2\pi(y - y_0)) - 2\cos(2\pi(x - x_0)) + 2\delta^2},
$$

i.e., $\mathbf{u}_{(x_0, y_0)}$ is the velocity field generated by a periodic vortex blob located at $\mathbf{x}_0 = (x_0, y_0)$. The x-average of the x-component of $\mathbf{u}_{(x_0, y_0)}$ can easily be determined by contour integration. It equals

$$
(74) \qquad \bar{u}_{(x_0, y_0)}(y) = -\frac{1}{2} \frac{\sinh(2\pi(y - y_0))}{\sqrt{(\cosh(2\pi(y - y_0)) + \delta^2)^2 - 1}}.
$$

For $y_0 > 0$, $s > y_0$, we have

$$
(75) \qquad \int_{-s}^{s} \bar{u}_{(x_0, y_0)}(y)\, dy = \int_{-s}^{-s + 2y_0} \bar{u}_{(x_0, y_0)}(y)\, dy.
$$

Thus,

$$
(76) \qquad \int_{-\infty}^{\infty} \bar{u}_{(x_0, y_0)}(y)\, dy := \lim_{s \to \infty} \int_{-s}^{s} \bar{u}_{(x_0, y_0)}(y)\, dy = y_0.
$$

Similarly, one sees that (76) is true when $y_0 < 0$. If

$$\text{(77)} \qquad \mathbf{u}(\mathbf{x}) = \sum_{i=1}^{m} \omega_i \mathbf{u}_{(x_i, y_i)}(\mathbf{x}),$$

we conclude that

$$\text{(78)} \qquad \int_{-\infty}^{\infty} \bar{u}(y, t)\, dy := \lim_{s \to \infty} \int_{-s}^{s} \bar{u}(y, t)\, dy = \sum_i \omega_i y_i.$$

Together with Eqs. (71) and (74), this shows:

LEMMA 2. *If*

$$\text{(79)} \qquad \sum_i \omega_i = 0,$$

then the velocity field defined by Eq. (77) has the x-momentum thickness

$$\text{(80)} \qquad \theta = \frac{\sum_i \omega_i y_i}{\sum_i \omega_i H_\delta(y_i)}$$

with

$$\text{(81)} \qquad H_\delta(y_i) := \frac{1}{2}\left(\frac{\sinh(2\pi y_i)}{\sqrt{(\cosh(2\pi y_i) + \delta^2)^2 - 1}} + 1 \right).$$

For $\delta = 0$, H_δ is the Heaviside function, and Eq. (80) is then identical with Eq. (18) of [2]. We apply Lemma 2 to the space discretized equations (see Section 3), which are ordinary differential equations for $\mathbf{x}_i(t) = (x_i(t), y_i(t))$, $i = 1, \ldots, N$. $\mathbf{x}_i(t)$ is a point on the positive vortex sheet $\mathbf{x} = \mathbf{x}_+$.

LEMMA 3. *The x-momentum thickness at time t of the solution of the space discretized equations is*

$$\text{(82)} \quad \theta(N, \delta, t) = \frac{2\sum_{i=1}^{N} y_i(t)}{\sum_{i=1}^{N} \frac{\sinh(2\pi y_i(t))}{\sqrt{(\cosh(2\pi y_i(t)) + \delta^2)^2 - 1}}} = \frac{2\sum_{i=1}^{N} y_i(0)}{\sum_{i=1}^{N} \frac{\sinh(2\pi y_i(t))}{\sqrt{(\cosh(2\pi y_i(t)) + \delta^2)^2 - 1}}}.$$

Proof. This follows from Lemma 2 because

$$\text{(83)} \qquad \frac{d}{dt}\sum_{i=1}^{N} y_i(t) \equiv 0.$$

Equation (83) easily follows from Eq. (68). □

10. Numerical Experiments. The numerical experiments presented in this section were carried out on a SUN 3/60 workstation, using double-precision arithmetic, i.e., approximately 16 decimal digits.

A change in Γ is equivalent with a scaling of the time. Therefore we take

$$\text{(84)} \qquad \Gamma = 1$$

without loss of generality. As a test example, we choose the problem of Figure 10 of [1]:

$$\text{(85)} \qquad x^{(0)}(\gamma) = \gamma - 0.025 \sin(2\pi\gamma),$$

and

(86) $$y^{(0)}(\gamma) = -0.12 + 0.025\sqrt{\tanh(0.24\pi)}\sin(2\pi\gamma).$$

We have used

(87) $$\delta = 0.1$$

for the experiments of this paper. This choice is more or less arbitrary. For $\delta = 0.1$, curves are obtained which we believe to be reasonable approximations of the solutions for $\delta = 0$; compare Figure 5 of [10].

We compute up to time $T = 1.5$. At this time, good resolution can still be obtained using a relatively small number of vortex blobs. Keeping the same numbers of vortex blobs as in the experiments described below, the errors would already be significantly larger at time $T = 2.0$. This deterioration of the spatial resolution as time progresses is not too surprising in view of the large increase in the arc lengths of the sheets. In [11], Krasny used an adaptive point insertion technique to continue his computations over a longer time interval.

Let $(x_i(N,t), y_i(N,t))$, $1 \le i \le N$, be the solution of the space discretized equations, and let $(x_i(N,t,\Delta t), y_i(N,t,\Delta t))$ be the numerical approximation to $(x_i(N,t), y_i(N,t))$ obtained using the classical Runge-Kutta method. We compare the approximations obtained on meshes of several different sizes with each other. More precisely, we define

(88) $$E(N,T,\Delta t) := \max_{i=1,\dots,N} \|\mathbf{x}_i(N,T,\Delta t) - \mathbf{x}_{2i}(2N,T,\Delta t)\|_2$$

and

(89) $$E(N,T) := \max_{i=1,\dots,N} \|\mathbf{x}_i(N,T) - \mathbf{x}_{2i}(2N,T)\|_2.$$

Numerically, we find:

(90) $$E(N = 20,\ T = 1.5,\ \Delta t = 0.05) = 0.1325,$$

(91) $$E(N = 20,\ T = 1.5,\ \Delta t = 0.025) = 0.1170,$$

(92) $$E(N = 20,\ T = 1.5,\ \Delta t = 0.0125) = 0.1167.$$

Thus we conclude

(93) $$E(N = 20,\ T = 1.5) \approx 0.12.$$

Table 1 shows approximate errors obtained in this way for various values of N.

TABLE 1

Errors in blob positions caused by space discretization.

N	20	40	80	160
$E(N, T = 1.5)$	1.2×10^{-1}	1.1×10^{-1}	5.4×10^{-2}	4.4×10^{-3}

We also consider the error in the momentum thickness,

(94) $$E_m(N,T,\Delta t) := \theta(N,T,\Delta t) - \theta(2N,T,\Delta t)$$

and

(95) $$E_m(N,T) := \theta(N,T) - \theta(2N,T),$$

where θ is defined by Eq. (82), and $\theta(N, T, \Delta t)$ is the approximation for

$$(96) \qquad \frac{2 \sum_{i=1}^{N} y_i(t)}{\sum_{i=1}^{N} \frac{\sinh(2\pi y_i(t))}{\sqrt{(\cosh(2\pi y_i(t)) + \delta^2)^2 - 1}}}$$

obtained with the time stepsize Δt. We find

$$(97) \qquad E_m(N = 20, \ T = 1.5, \ \Delta t = 0.05) = -6.589 \times 10^{-3},$$

$$(98) \qquad E_m(N = 20, \ T = 1.5, \ \Delta t = 0.025) = -6.407 \times 10^{-3},$$

$$(99) \qquad E_m(N = 20, \ T = 1.5, \ \Delta t = 0.0125) = -6.407 \times 10^{-3}.$$

Thus we conclude

$$(100) \qquad E_m(N = 20, \ T = 1.5) \approx -6.41 \times 10^{-3}.$$

Table 2 shows approximate errors obtained in this way for various values of N.

TABLE 2

Errors in momentum thickness caused by space discretization.

N	20	40	80	160
$E_m(N, T = 1.5)$	-6.4×10^{-3}	1.3×10^{-2}	-4.2×10^{-3}	-7.7×10^{-4}

This illustrates the accuracy with which the space discretized equations approximate the continuous regularized Birkhoff equations. We shall now consider the error caused by the time discretization. We define

$$(101) \qquad \mathscr{E}(N, T, \Delta t) := \max_{i=1,\dots,N} \left\| \mathbf{x}_i(N, T, \Delta t) - \mathbf{x}_i\left(N, T, \frac{\Delta t}{2}\right) \right\|_2$$

and

$$(102) \qquad \mathscr{E}_m(N, T, \Delta t) := \theta(N, T, \Delta t) - \theta\left(N, T, \frac{\Delta t}{2}\right).$$

Tables 3 and 4 show $\mathscr{E}(N, T = 1.5, \Delta t = 0.0125)$ and $\mathscr{E}_m(N, T = 1.5, \Delta t = 0.0125)$ for various values of N. The main conclusion here is that for $\Delta t = 0.0125$, the errors caused by the time discretization are negligible in comparison with the errors caused by the space discretization, for the values of N which we have used.

TABLE 3

Errors in blob positions caused by time discretization, $\Delta t = 0.0125$.

N	20	40	80	160
$\mathscr{E}(N, T = 1.5, \Delta t = 0.0125)$	5.7×10^{-5}	7.8×10^{-5}	2.8×10^{-5}	1.6×10^{-5}

TABLE 4

Errors in momentum thickness caused by time discretization, $\Delta t = 0.0125$.

| N	20	40	80	160
$\mathscr{E}_m(N, T = 1.5)$	8.1×10^{-8}	1.4×10^{-7}	1.6×10^{-8}	2.9×10^{-9}

11. Figures. For illustration, we show pictures of a solution of the regularized Birkhoff equations with $\delta = 0.1$. Our figures show the evolution of sheets with the initial conditions (85), (86), computed using
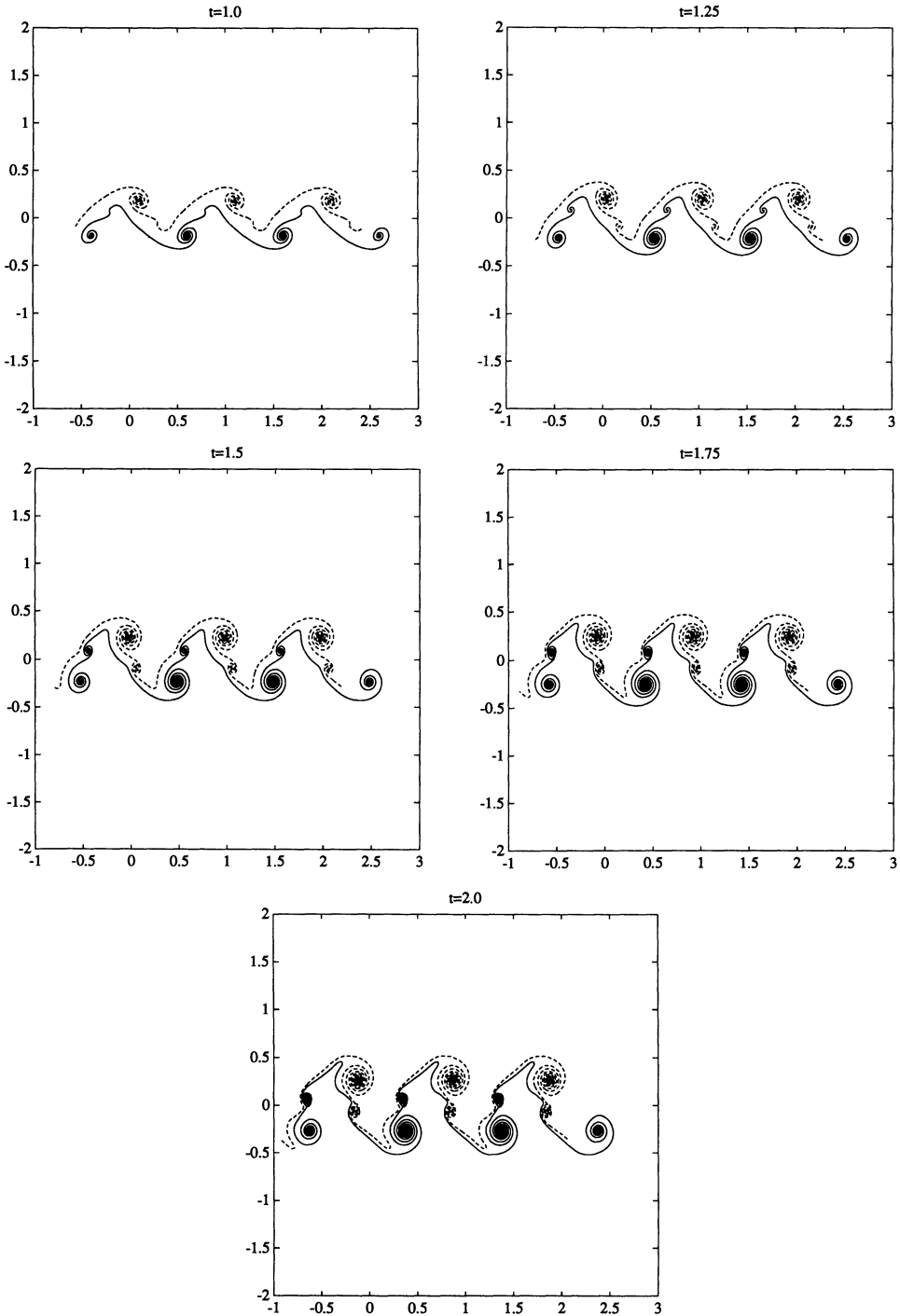
$$(103) \qquad\qquad N = 400$$

and

$$(104) \qquad\qquad \Delta t = 0.00625.$$

The plotted curves interpolate the computed points piecewise cubically. The tangling of the curve at time $t = 1.75$ is an effect of the finiteness of N.
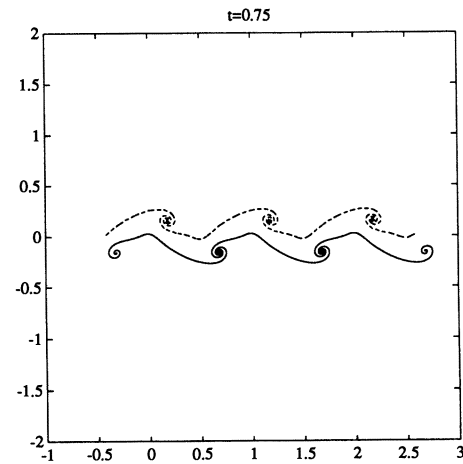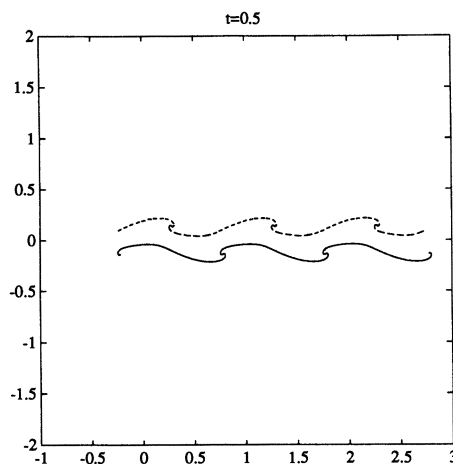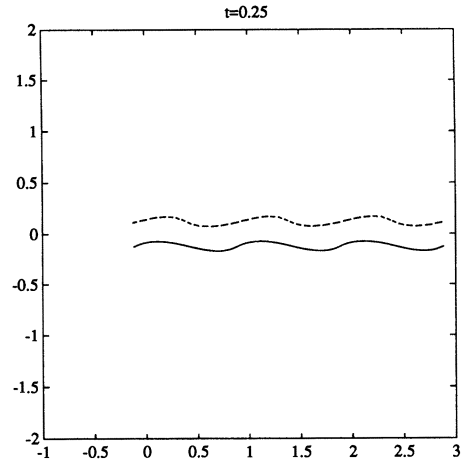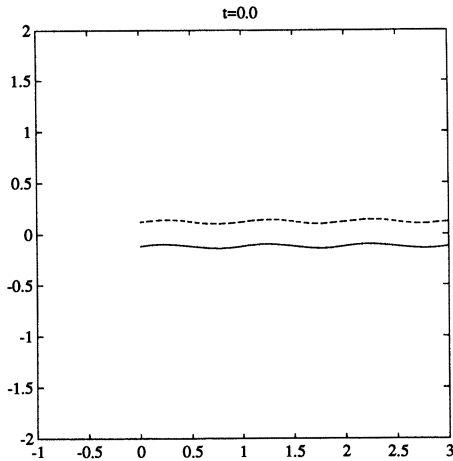
12. Concluding remarks. Our considerations can briefly be summarized as follows: Nothing goes wrong as long as the regularization parameter δ is fixed. The continuous problem is harmless (Theorems 1, 2 and 6), the space discretized problem is harmless (Theorem 3), the errors caused by space discretization are of the expected order (Theorems 4 and 5), and the error caused by time discretization is small independently of the space mesh size (Theorem 7).

We shall conclude with a few remarks about the limit $\delta \to 0$, which was studied, for small T, by Caflisch and Lowengrub [5]. First consider the constants $C = C(T, \mu, \delta, m)$ and $L = L(\delta, m)$ of Theorems 4 and 5. As $\delta \to 0$, these constants are expected to grow. The reason is that the solutions become more complicated as δ decreases, so that smaller values of h are required to achieve a prescribed accuracy. I do not know whether the factor in front of h^{μ_0} in Eq. (34) tends to infinity as $\delta \to 0$. If μ_0 is replaced by 1, and if T is sufficiently small, then estimate (b) of Theorem 2 in [5] shows that the factor remains bounded as $\delta \to 0$.

Next consider the constant $D = D(T, \delta)$ in Eq. (54). From numerical experiments it appears that D grows rapidly as $\delta \to 0$. Again, I do not know whether this growth is bounded as $\delta \to 0$. For sufficiently small T, a closely related bound is given by estimate (c) of Theorem 2 in [5].

For small δ, roundoff errors become important. This was pointed out and studied in detail by Krasny [10]. Compare also Eq. (2.18) of [5], which suggests that for analytic initial data and short time, errors caused by roundoff roughly grow like $\max(e^{\rho/h}, e^{\rho/\delta^2})$ as $\delta \to 0$, $h \to 0$, with a constant $\rho > 0$ dependent on the initial data. However, Krasny [10] has proposed and tested a filtering technique which overcomes the problems related to rounding.

Department of Mathematics
University of Michigan
Ann Arbor, Michigan 48109
E-mail: Christoph_Borgers@um.cc.umich.edu

1. F. H. ABERNATHY & R. E. KRONAUER, "The formation of vortex streets," *J. Fluid Mech.*, v. 13, 1962, pp. 1–20.

2. H. AREF & E. D. SIGGIA, "Evolution and breakdown of a vortex street in two dimensions," *J. Fluid Mech.*, v. 109, 1981, pp. 435–463.

3. G. BIRKHOFF, *Helmholtz and Taylor Instability*, Proc. Sympos. Appl. Math., vol. 13, Amer. Math. Soc., Providence, R. I., 1962, pp. 55–76.

4. D. R. BOLDMAN & P. F. BRINICH & M. E. GOLDSTEIN, "Vortex shedding from a blunt trailing edge with equal and unequal external mean velocities," *J. Fluid Mech.*, v. 75, 1976, pp. 721–735.

5. R. CAFLISCH & J. LOWENGRUB, *Convergence of the Vortex Method for Vortex Sheets*, Preprint, 1988.

6. R. CAFLISCH & O. ORELLANA, "Long-time existence for a slightly perturbed vortex sheet," *Comm. Pure Appl. Math.*, v. 39, 1986, pp. 807–838.

7. A. J. CHORIN, "Numerical study of slightly viscous flow," *J. Fluid Mech.*, v. 57, 1973, pp. 785–796.

8. C. W. GEAR, *Numerical Initial Value Problems in Ordinary Differential Equations*, Prentice-Hall, Englewood Cliffs, N. J., 1971.

9. R. KRASNY, "A study of singularity formation in a vortex sheet by the point-vortex approximation," *J. Fluid Mech.*, v. 167, 1986, pp. 65–93.

10. R. KRASNY, "Desingularization of periodic vortex sheet roll-up," *J. Comput. Phys.*, v. 65, 1986, pp. 292–313.

11. R. KRASNY, "Computation of vortex sheet roll-up in the Trefftz plane," *J. Fluid Mech.*, v. 184, 1987, pp. 123–155.

12. E. MEIBURG, "On the role of subharmonic perturbations in the far wake," *J. Fluid Mech.*, v. 177, 1987, pp. 83–107.

13. D. W. MOORE, "The spontaneous appearance of a singularity in the shape of an evolving vortex sheet," *Proc. Roy. Soc. London Ser. A*, v. 365, 1979, pp. 105–119.

14. C. SULEM, P. L. SULEM, C. BARDOS & U. FRISCH, "Finite time analyticity for the two-